

# Modeling a Lightweight Deflectometer Test of Unbound Granular Materials with the Discrete Element Method

Jian Wang\*, Member, IAENG, Aimin Sha, Liqun Hu, and Wei Jiang

**Abstract**—Unbound granular materials are widely used in the base and subbase layers of pavement systems. Currently, the compaction quality assurance (QA) of unbound granular base is mostly density-based with many drawbacks and is to be replaced by modulus-based QA. The Light Weight Deflectometer (LWD) test, which is often used to determine the stiffness of unbound granular materials, is a promising tool for modulus-based compaction QA but needs a more fundamental understanding of its experimental configuration and data interpretation. We build a digital model that adopts a discrete element method to model LWD field tests and account for the effects of moisture and finer particles by adopting a modified Hertz contact model which includes a component of attractive force. We investigate the relations between microscopic parameters and macroscopic material properties qualitatively, finding that the LWD modulus increases with model suction which is reversely related to moisture content, or interparticle friction which is reversely related to fine content. We calibrate this model using test results from field LWD tests. From the modeling results, we observe a trend of decreasing stiffness with increasing moisture or fine particle content, which agrees with existing experimental data. With the quantitative relations obtained from calibration, the model can be used to predict the LWD modulus of unbound granular base.

**Index Terms**—discrete element modeling, lightweight deflectometer, pavement engineering, unbound granular base

## I. INTRODUCTION

THE good flexibility and cost effectiveness of unbound granular materials have led to their widespread use in the base and subbase layers of pavement systems, especially in cold regions [1]. The strength, stiffness and stability of the unbound granular base is therefore crucial to pavement systems' performance and service life. Due to the complex behaviors of unbound granular base under vehicle load, such as shear dilatancy, non-linearity and cross-anisotropy [2], [3], it is critical to characterize the deformation of unbound base material properly with results from both laboratory and field

tests.

On one hand, the widely accepted laboratory test for the characterization of unbound granular materials is the cyclic load triaxial (CLT) test in which the vehicle load is simulated by cyclic deviator stresses [4]. The resulting strains from CLT tests are often used to calculate the resilient modulus which is a fundamental input for mechanical-empirical pavement design procedure and is considered the most important property of unbound granular material [5].

On the other hand, in field testing, compaction quality assurance (QA) is usually based on density rather than modulus because soil density can be easily measured and is loosely related to more fundamental engineering properties. For example, the Chinese specification requires the dry density of the base to reach a certain percentage of the maximum dry density (degree of compaction). However, density is not a direct input parameter for pavement design, nor is it directly related to pavement performance. Moreover, the particle arrangement in the soil structure may be very different in the absence of a significant difference in dry density, resulting in different properties and behavior of the soil [6].

Therefore, in recent years, modulus-based compaction QA is gaining attention in the pavement industry. The Lightweight Deflectometer (LWD) test is one of the most promising techniques for modulus-based QA. The LWD is a portable device that can be used to directly measure the surface modulus of an unbound layer in the field. It is currently being employed for pavement construction QA in some states in the United States. In China, it is usually used to complement the conventional density-based QA [7]. However, due to the lack of widely accepted standards to interpret the measured stiffness data, its broader implementation has been hampered. There are significant challenges in establishing a standard specification, including differences in the configuration of various commercial LWD devices, non-linearity of the soil modulus under different moisture and stress conditions, and the differences in the stress states and boundary conditions between typical laboratory tests and field conditions [8]. To use the LWD test with methods based on the modulus QA specification to replace the traditional density-based QA, fundamental understanding of the experimental configuration and data interpretation of the LWD test is required.

The discrete element method (DEM), a discontinuous method capable of simulating individual particles and detailed interparticle interactions during material deformation, can provide insights into unbound granular material behavior at particle level [9]–[12]. The contact model imposed on interparticle contacts has a significant influence on the material response under load [13], [14].

Manuscript received April 24, 2018; revised July 18, 2018.

\*Jian Wang, corresponding author, is with the School of Highway, Chang'an University, Xi'an, Shaanxi, 710064, and School of Civil and Transportation Engineering, Henan University of Urban Construction, Pingdingshan, Henan, 467000, China, e-mail: jianwang0712@gmail.com.

Aimin Sha is with the Key Laboratory for Special Area Highway Engineering of Ministry of Education, Chang'an University, Xi'an, Shaanxi, 710064 China.

Liqun Hu is with the Key Laboratory for Special Area Highway Engineering of Ministry of Education, Chang'an University, Xi'an, Shaanxi, 710064 China.

Wei Jiang is with the Key Laboratory for Special Area Highway Engineering of Ministry of Education, Chang'an University, Xi'an, Shaanxi, 710064 China.

Water bridge forces may be incorporated into the contact model to simulate wet granular material, resulting in an increase in bulk modulus [15], [16]. This type of contact model is necessary for simulation of unbound granular base material since capillary water usually exists in such materials. The relation between water bridge forces and experimental soil suction needs further investigation.

This paper employs the discrete element method to simulate the LWD test of the unsaturated aggregates of a specific gradation (G-A-5). A Hertz model with attraction force is used as a contact model to account for the effects of moisture and fines. Qualitative analysis is performed to explore the connections between micro and macro properties. We also used published test results to develop quantitative relations between virtual and physical testing parameters, which can be used for calibrating virtual LWD tests from field data. With these virtual LWD tests, a better understanding of LWD test configuration and contact model effects on the material responses (for example, LWD modulus) may be obtained. Moreover, we present an easy-to-use, less computationally demanding calibration procedure for obtaining the quantitative relationships between test and simulation results. Ultimately, the goal is to gain insight into the underlying mechanism of granular material deformation under LWD loading conditions and to partly replace physical tests with virtual LWD tests.

## II. LWD FIELD TEST

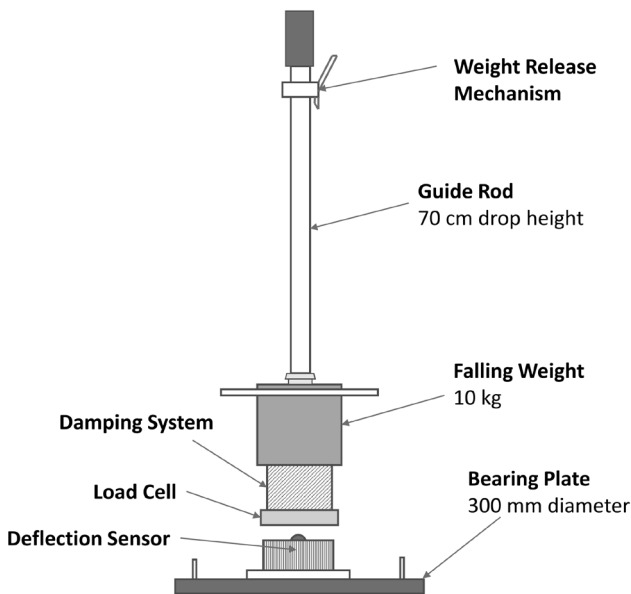


Fig. 1. Structure of a typical LWD instrument

A typical LWD test device is shown in Fig.1. It contains a drop weight as a loading mechanism. Once released, the weight falls along a rod until it hits a disk-shaped bearing plate which is in contact with the ground. Once the drop weight hits the plate, the LWD and ground move together in contact with each other. A pulse load is generated and applied to underlying soil via the plate. The weight and the plate lose contact when the impact load becomes zero. A velocity sensor or accelerometer records the speed or acceleration of the movements of the ground. The whole LWD-ground system can be represented by a two degrees of freedom

(DOF) mass-spring-damper system, and the maximum displacement can be calculated by means of double/single integrations of the accelerations/velocities. During the test, the load history and peak load are measured by a load cell.

Usually, several drops are carried out on the same testing spot; the first few drops are typically discarded. The average deflections from subsequent drops are used to calculate an effective modulus.

The LWD value can be expressed by peak deflection  $\Delta$  or the effective bulk modulus  $E_{LWD}$ . According to Davich et al. [17],  $E_{LWD}$  can be calculated by:

$$E_{LWD} = 2r_p\sigma(1-\nu_s^2)\frac{10^6 D}{\Delta} \quad (1)$$

where  $\Delta$  is the measured peak deflection,  $r_p$  the radius of the LWD plate,  $\sigma$  the peak stress applied on the LWD plate,  $\nu_s$  the Poisson's ratio of the bulk granular material, and  $D$  the stiffness of the LWD plate.

Field test results show that LWD values vary with moisture and particle size distribution [18]. The former can be represented by gravimetric moisture content  $\omega_g$  and the latter by grading number GN:

$$\omega_g = \frac{m_w}{m_s} \quad (2)$$

$$GN = \frac{(\sum p_{ss})\%}{100\%}$$

where  $m_w$  is the mass of water,  $m_s$  the mass of dry granular material,  $p_{ss}$  the percent passing specific sieve size by weight. It should be noted that GN is a non-unique measure of size distribution. In general, mixtures with a higher fraction of smaller particles tend to have a higher GN.

For a given particle size distribution or GN, as the water content increases, the peak deflection increases and the corresponding effective bulk modulus decreases. Additionally, for a given water content, peak deflection  $\Delta$  increases with GN, thus decreasing the effective bulk modulus [18]. Similar trends can be obtained from simulated LWD tests. Before elaborating on the details of modeling an LWD test, we first introduce the basic concepts of DEM modeling and the contact model used in the next section.

## III. DISCRETE ELEMENT METHOD

### A. Fundamentals of DEM

The DEM is an explicit time stepping algorithm that applies Newton's second law of motion [19]. In the DEM simulation, it is assumed that particles are rigid bodies, and interparticle deformations are very small and thus can be simplified as interparticle overlaps. The time step is small enough that the velocities and accelerations of particles can be treated as constant values during each time step. Then, the interparticle contact forces and moments are calculated by contact laws, with interparticle overlaps and parameters associated with particle material properties as inputs.

Rotations and velocities of particles conform to Newton's second law. The simulation starts from an assembly of particles with known grain material properties, geometries,

initial positions and velocities. By inputting the material properties, interparticle velocities and the interparticle overlaps to the contact law, the interparticle forces and moments can be solved. Then, the resultant interparticle forces and moments are substituted into Newton's second law to obtain the updated velocities and positions by time step integration. Cycle by cycle, the deformation (e.g., a triaxial shearing) of a granular material assembly can be simulated. This demonstrates the connection between the microscopic forces and the macroscopic granular material behaviors for geomechanics research. In this study, classical general-purpose DEM software called PFC3D (Particle Flow Code in 3 Dimensions) is employed.

### B. The Hertz Contact Model

For a typical DEM model, the macroscopic granular material behaviors depend heavily upon the interparticle contact model. In this study, we utilize a three-dimensional contact model which is based on Hertz-Mindlin contact theory [20]. It consists of a nonlinear stiffness component, a damping component and Coulomb sliding friction. The normal contact force  $F_n$  and shear contact force  $F_s$  are updated each cycle according to the following equations:

$$\begin{aligned} F_n &= -k_n \delta_o^{\frac{3}{2}} - \eta_n \delta_o^{\frac{1}{4}} \dot{\delta}_o \\ F_s &= \min \left\{ -k_s \delta_o^{\frac{1}{2}} \delta_s - \eta_s \delta_o^{\frac{1}{4}} \dot{\delta}_s, \mu F_n \right\} \\ \text{with } \dot{\delta}_o &= \frac{d\delta_o}{dt}, \quad \dot{\delta}_s = \frac{d\delta_s}{dt} \end{aligned} \quad (3)$$

where  $\delta_o$  is the contact overlap ( $\delta_o > 0$  is overlap) and  $\dot{\delta}_o$  is the relative translational velocity normal to the contact plane defined such that  $\dot{\delta}_o > 0$  is increasing overlap.  $\delta_s, \dot{\delta}_s$  are relative displacement and velocity tangent to the contact plain, respectively,  $k_n, k_s$  are normal and shear stiffness coefficients, and  $\eta_n, \eta_s$  are normal and shear damping coefficients.  $k_n, k_s, \eta_n, \eta_s$  are derived from the effective properties of contact. The stiffness coefficients  $k_n$  and  $k_s$  are given by:

$$\begin{aligned} k_n &= \frac{4}{3} E_e \sqrt{R_e} \\ k_s &= 8G_e \sqrt{R_e} \end{aligned} \quad (4)$$

with:

$$\begin{aligned} R_e &= \left( \frac{1}{R_1} + \frac{1}{R_2} \right)^{-1}, \quad E_e = \left( \frac{1-\nu_1^2}{E_1} + \frac{1-\nu_2^2}{E_2} \right)^{-1} \\ G_e &= \left( \frac{2(1+\nu_1)(2-\nu_1)}{E_1} + \frac{2(1+\nu_2)(2-\nu_2)}{E_2} \right)^{-1} \end{aligned}$$

where  $R_e, E_e$ , and  $G_e$  are the effective radius, the effective Young's modulus, and the effective shear stiffness at the point of contact between particles 1 and 2.  $R_{\{1,2\}}, E_{\{1,2\}}$ , and  $\nu_{\{1,2\}}$  are the radius, Young's modulus, and Poisson's ratio of the two particles in contact, respectively.

The damping coefficients are determined by:

$$\begin{aligned} \eta_n &= \alpha_h \sqrt{m_e k_n}, \\ \eta_s &= \alpha_h \sqrt{m_e k_s} \end{aligned} \quad (5)$$

with:

$$m_e = \left( \frac{1}{m_1} + \frac{1}{m_2} \right)^{-1},$$

where  $m_e$  is the effective mass of contact,  $m_{\{1,2\}}$  represents particle mass and  $\alpha_h$  is the damping constant, which is related only to the coefficient of restitution.

### C. Modeling Moisture Force

To account for moisture effects, a moisture force, which is an interparticle attractive force, is added to the above-mentioned Hertz contact model. The modified Hertz model has two moisture states, dry and wet, corresponding to dry granular material and wet granular material respectively. When the moisture state is wet, moisture force  $F^m$  is added to the contact model. The moisture force model originated from the liquid bridge model, which mechanistically captures the effect of interparticle dispersed liquid on the macroscopic response of the bulk material [21]. The liquid bridge model does not capture the moisture effect when finer particles are present whereas the modified Hertz model employed in this paper does.

For wet granular material, the moisture force, which is defined as an attractive force acting on the normal of the contact plane, is maximal when two particles are in contact or overlapping. The moisture force decays exponentially as the distance between particle surfaces in contact – called the contact gap ( $g_c, g_c < 0$  indicates overlapping) – increases. When the contact gap reaches a critical distance of  $2s_{cr}$ , the liquid bridge ruptures and the moisture force becomes zero. Generally, the moisture force  $F^m$  can be summarized by following equation:

$$F^m = \begin{cases} F_{\max}^m & , g_c < 0 \\ F_{\max}^m \exp\left(\frac{-g_c}{2s_{cr}}\right) & , 0 \leq g_c \leq 2s_{cr} \\ 0 & , g_c > 2s_{cr} \end{cases} \quad (6)$$

$$\begin{aligned} \text{with } F_{\max}^m &= \psi(\pi R_o^2), \\ s_{cr} &= R_o = \min(R_1, R_2). \end{aligned}$$

where  $F_{\max}^m$  is the maximum moisture force determined by model suction ( $\psi$ ) and the minimal radius of contact particles ( $R_o$ ).

One of the most important input parameters for the modified Hertz model is the model suction parameter  $\psi$  (stress unit), which can be estimated from soil suction obtained from physical tests for the SWCC (soil-water characteristic curve). The choice of suction values is discussed in the next section.

IV. SIMULATION OF UNSATURATED GRANULAR SOIL

A. Particle Size Distribution

The coarse particles in granular material can be explicitly modeled; the material properties and gradation of coarse particles can be directly input as model parameters. However, as the number of particles increases, the computational demands of the model increase dramatically. Hence, it is not feasible to model finer particles explicitly. Therefore, the finer particles are not generated in the DEM model; their effect on the system is simulated by the contact model.

TABLE I  
G-A-5 GRADATION FROM THE SPECIFICATION

Sieve Size (mm))	Percent Passing (%)
26.5	100
19	95-100
16	82-89
13.2	70-79
9.5	53-63
4.75	30-40
2.36	19-28
1.18	12-20
0.6	8-14
0.3	5-10
0.15	3-7
0.075	2-5

A Chinese specification titled, “Road Pavement Construction Technical Specification (JTG/T F20-2015)” recommends using several particle size distributions in the base layer of pavement. Here we focused on the G-A-5 gradation (Table I).

TABLE II  
G-A-5 GRADATION AS REPRESENTED IN THE DEM MODEL

Sieve Size (mm)	Percent Passing	Particle Size (mm)	Percent in Range (%)
26.5	100	19.0-26.5	5
19.0	95	16.0-19.0	13
16.0	82	13.2-16.0	12
13.2	70	9.5-13.2	17
9.5	53	4.8-9.5	23
4.8	30	≤4.75	30

The particle sizes in G-A-5 gradation range from less than 0.075 mm to 26.5 mm. Particle sizes greater than 4.75 mm can be modeled explicitly. To reduce the number of particles—and thus computational demand—particles smaller than 4.75 mm are not modeled explicitly and are partly accounted for by contact models. The modified gradation used in the DEM simulation, which is based on the G-A-5 gradation, is shown in Table II.

B. Suction  $\psi$  and Friction Coefficient  $\mu$

Since the tests used to obtain the suction of unsaturated soil are expensive and time-consuming, we used existing test results to estimate suction  $\psi$  in this model. Gupta and Larson [22] studied mixtures of sand, silt, clay, and organic matter at different water contents and proposed an empirical relationship between the volumetric water content and percentages of these ingredients. Their experimental moisture content covers the range of water content typically

found in unbound granular bases (about 10%). For the mixture of sand and silt, the empirical relationship can be written as:

$$\theta_p = a \times \text{sand}\% + b \times \text{silt}\% + c \times \rho_b \quad (7)$$

where  $\theta_p$  is the volumetric moisture content.  $\rho_b$  is the bulk density of the mixture, and  $a, b, c$  are empirical coefficients.

The coefficients of each item in (7) are functions of suction. The test results can be fitted with the least-squares method to obtain the empirical suction corresponding to different volumetric water contents  $\theta_p$ . Table III shows empirical suction values calculated from various combinations of  $\theta_p$  and silt content.

Note that the larger particle in Gupta’s test is sand, with an average particle size of approximately 2 mm; the representative particle size (mass weighted average) of the DEM model is 12 mm. Applying the dynamic similarity between the physical test and DEM simulation, the model suction is six times the empirical suction. The model suction values are also shown in Table III.

TABLE III  
G-A-5 GRADATION FROM THE SPECIFICATION

$\theta_p$ (%)	Silt Content (%)	Empirical Suction (kPa)	$\psi$ (kPa)
10	10	50	300
15	30	50	300
15	20	23	138
15	10	11	66
20	30	16	96
20	20	8.3	50
20	10	5.5	33

The suction parameter  $\psi$  considers the effects of moisture, but not the effects of finer particles. With the modified Hertz model, such a simulation is mainly achieved by (1) allowing moisture forces to exist between contacting particles within a certain distance (the moisture gap,  $g_c$ ,  $g_c > 0$ ) when the moisture is first added (i.e., when the moisture state becomes wet) so that we can simulate suction in finer particles that fill the pores between coarse particles; (2) varying the interparticle friction coefficient  $\mu$ . Smaller interparticle frictions can be used to simulate the stabilization or lubrication effect of finer particles between coarse particles. In this study, we simulate different finer particle contents mainly by varying the friction coefficient between particles to values of 0.2, 0.3, and 0.4.

C. Other Modeling Parameters

The material properties of granite are used as particle material properties. The values of Young’s modulus, Poisson’s ratio, and density are 29 GPa, 0.15, and 2650 kg/m<sup>3</sup>, respectively. For the LWD plate, we used the material properties of steel, which has a Young’s modulus, Poisson’s ratio, and density of 210 GPa, 0.30, and 7850 kg/m<sup>3</sup>, respectively. Damping ratio  $\alpha_n$  in (5) is set to 0.07, corresponding to a coefficient of restitution of 90%. In

addition, the local damping of particles is set to 0.7 to keep the system quasi-static.

## V. SIMULATION OF LWD TEST PROCEDURES

In the DEM simulation of an LWD field test, the load was applied to a steel plate 20 cm in diameter, so that the steel plate was subjected to a peak stress of 0.2 MPa. It is not possible to explicitly simulate the half-space body of the entire granular material. Instead, we adopted a cylindrical container 260 mm in diameter filled with spherical particles, which is large enough to avoid size constraint effects without excessively increasing the number of particles.

### A. Specimen Preparation

Before generating granular material for the LWD test, we first made a cylindrical vessel (Fig. 2). Next, we applied a boundary-contraction packing procedure [23] to the material using the following stages:

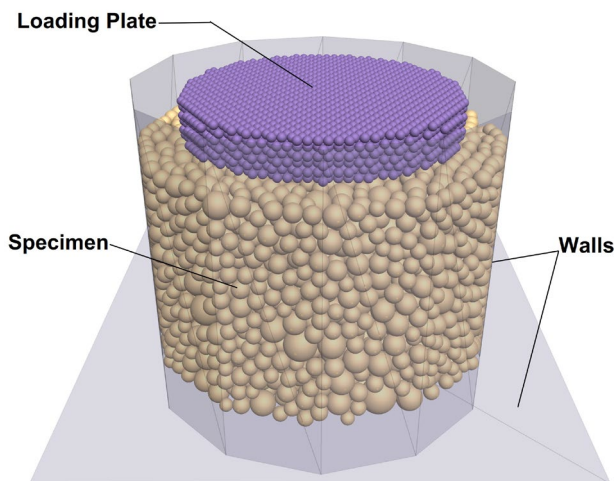


Fig. 2. Simulation of LWD loading. The loading plate is a clump consisting of closely packed balls. Boundaries are massless walls whose positions are fixed.

1. Generate a particle cloud with specific porosity. The porosity here does not account for the overlap between particles. The particles are generated according to a given grading and the location is randomly chosen; thus, large overlaps between particles are to be expected.
2. Set the particle friction coefficient to zero, which allows the particles to be rearranged until the average stress approaches zero or static balance is achieved. This step eliminates the large overlap between particles.
3. Set the particle friction coefficient to the specified value  $\mu_0$ , and apply confining pressure to the material.

During the confining stage, boundaries move under the control of a servomechanism until the boundary-measured pressure reaches a target value (within a specified tolerance) and static equilibrium is reached.

At the beginning of stage 3, the interparticle friction was set to a specified value temporarily so that we can obtain various initial packing configurations by altering  $\mu_0$ . Generally, under the same confining conditions, a denser

initial packing can be achieved by using a smaller  $\mu_0$ . In this paper, a friction coefficient of  $\mu_0 = 0.2$  was used for all simulated LWD tests to achieve the same dense initial packing.

We then introduced moisture and fines by adding a moisture force corresponding to suction value  $\psi$  and set the interparticle friction coefficient to  $\mu$ . While adding moisture, new contacts may be created. The moisture gap  $g_m$  was used to control the generation of interparticle contacts. New contacts were created only when the distance between contacting particles was smaller than the moisture gap  $g_m$ , which was arbitrarily chosen to be 1 mm for all simulations.

Note that another material genesis approach used by many is the gravitational settlement approach, in which randomly generated particles are allowed to settle under gravity and are compacted by external forces to obtain a dense packing [24]. By comparison, a boundary contraction approach is less computationally expensive, since it does not require a separate compaction stage. As described above, by applying a small interparticle friction, a compacted specimen can be obtained at the end of the boundary contraction procedure.

### B. LWD Loading

The LWD plate was modeled as a cylindrical clump consisting of mono-sized, hexagonal packed particles to form the so-called hexagonal closed-pack (HCP). The clump particle size is smaller than the smallest specimen particle size to make the load distribute uniformly (Fig. 2). Particle interactions within the clump were neglected. To reduce the complexity and calculation time of the model, loading was simplified to a pulse load applied to the plate. Within a short time, the load increased linearly from zero to a peak of 0.2 MPa and then linearly decreased to zero and remained in that state until a static equilibrium was reached.

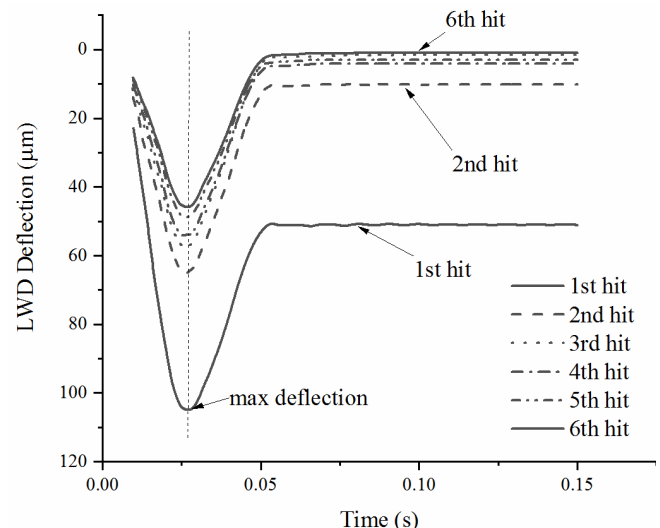


Fig. 3. Recorded deflections of six consecutive hits (with model suction  $\psi = 33$  kPa, interparticle friction  $\mu = 0.2$ ).

The relative position of the plate was recorded during loading. Fig. 3 shows the typical deflection results of an LWD test. The largest peak deflection appeared at the first impact and as the number of impacts increased, the peak deflection decreased. This is analogous to the change in the

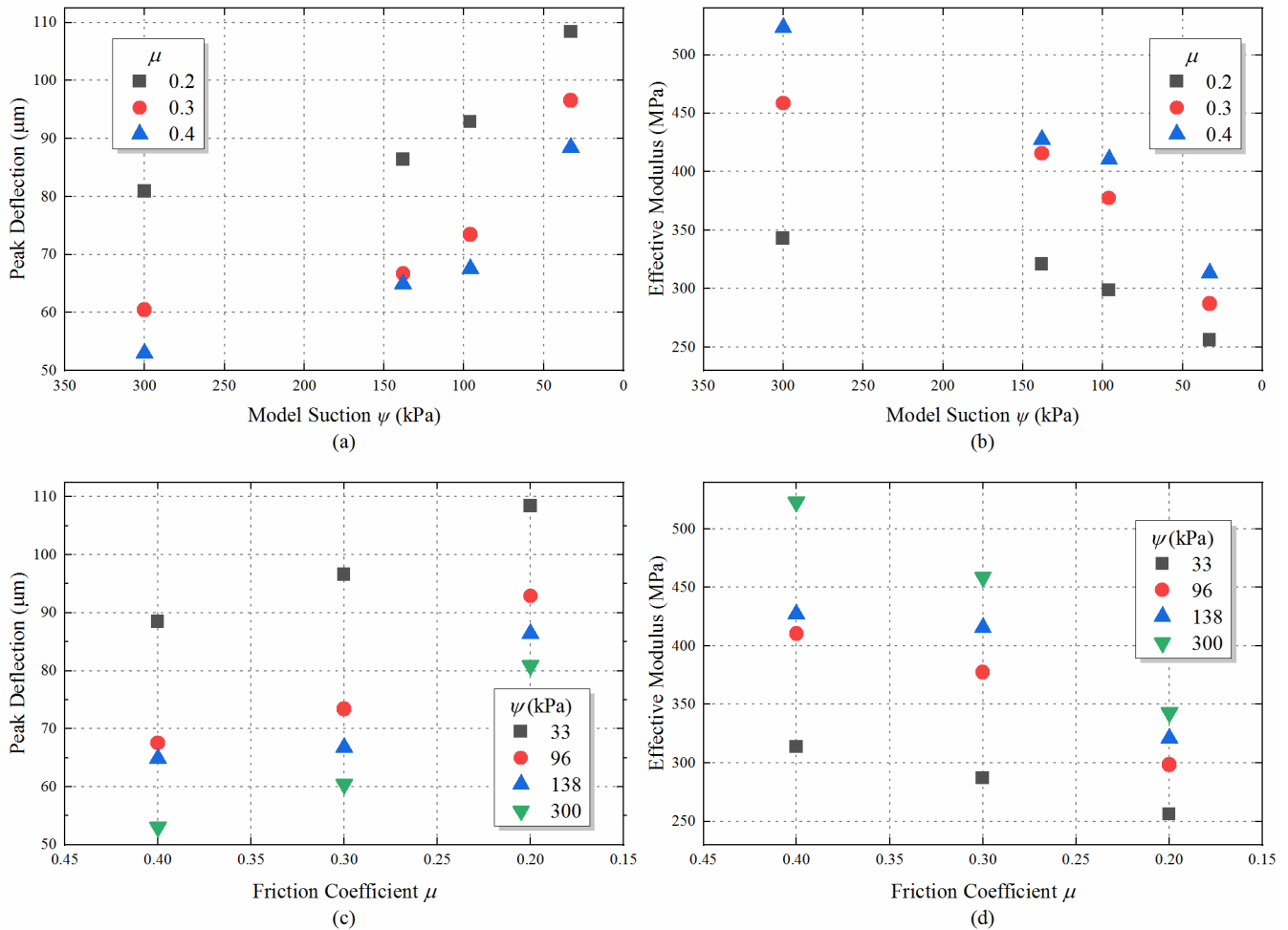


Fig. 4. LWD test results for DEM simulation: (a) peak deflection and (b) effective modulus plotted as functions of DEM Model suction  $\psi$ ; (c) peak deflection and (d) effective modulus plotted as functions of friction coefficient.

permanent strain observed in a typical laboratory CLT test, which decreases as loading number increases, but the overall permanent strain keeps increasing [25]. As with the LWD field test, the effective modulus of the granular material  $E_{\text{LWD}}$  was calculated from the average peak deflection from several consecutive drops [using (2) with  $r_p = 0.1 \text{ m}$ ,  $\sigma = 0.2 \text{ MPa}$ ,  $\nu_s = 0.35$ , and  $D = 0.79$ ]. The first three drops were discarded, and the deflections from subsequent drops were used to calculate the bulk modulus.

## VI. MODELING RESULTS

### A. Qualitative Analysis

A series of simulated LWD tests were carried out on the wet granular material prepared with the aforementioned procedure. The interparticle suction and frictions were varied so that we could demonstrate the relations between LWD values and the microscopic parameters. From Fig. 4 (a) and (b) we can clearly see that the peak deflection increased, and the corresponding bulk modulus decreased, with decreasing model suction  $\psi$ . As previously mentioned, the model suction  $\psi$  was related to the SWCC test results and decreased with increasing moisture content. Thus, it is safe to conclude that the peak deflection increased and the LWD modulus decreased with increasing moisture content, which agrees with reported field test results.

Similarly, Fig. 4 (c) and (d) shows that the peak deflection increases and corresponding LWD modulus decreases with decreasing interparticle friction. The interparticle friction can be related to fine content and a lower friction value indicates higher fine content in the mixture. In other words, the peak deflection increases and the LWD modulus decreases with increasing fine content, which, again, agrees with results observed in field tests.

From Fig. 4, it is clear that the deformation behavior of the modeled unbound granular material under LWD loading is significantly related to interparticle friction and model suction. Specifically, a nonlinear relationship between LWD modulus, interparticle friction and model suction is to be expected. To obtain a quantitative relationship, the DEM model should be calibrated properly with test results. In the next section, we present the calibration procedure and the calibrated modeling results.

### B. Calibration of DEM Parameters

As shown in the previous section, the simulation results captured trends from the test results. However, since the model parameters representing moisture and fine particles are not mechanically related to their physical entities, it was necessary to develop an appropriate model parameter calibration procedure to predict the LWD test results. To simplify this calibration, we assumed that the moisture content was solely determined by model suction  $\psi$ , whereas

the fine particle content and corresponding GN were solely determined by interparticle friction coefficient  $\mu$ . According to the test results, the relationship between the LWD deflection and test parameters was linear. Hence, we assumed that the relationship between the LWD deflection and model parameters was also linear. Through trial and error, we found a linear relationship between LWD deflection,  $1/\mu^2$ , and  $1/\ln\psi$ .

Using the least-squares method, we fitted the field test results to acquire the following equation:

$$\Delta_{\text{expt}} = 122 + 100(\text{GN} - 3) + 46.3(\omega_g). \quad (8)$$

Similarly, we obtained a linear relationship between LWD deflection,  $1/\mu^2$ , and  $1/\ln\psi$ :

$$\Delta_{\text{DEM}} = -5.73 + \frac{1.27}{\mu^2} + \frac{299.47}{\ln\psi}. \quad (9)$$

Comparing the test and modeling results, the peak deflection from the field test was generally about 5.2 times that from the model:

$$\Delta_{\text{expt}} \approx 5.2\Delta_{\text{DEM}}. \quad (10)$$

From (8), (9) and (10), we derived the following calibration equations:

$$\text{GN} \approx \frac{0.05}{\mu^2} + 3.19, \quad (11)$$

$$\omega_g = 1.46 + \frac{25.87}{\ln\psi}. \quad (12)$$

Fig. 5 shows the calibrated modeling results and field test results. They are in good agreement, except the modeling results cover only a subset of the field testing results when the data is plotted against GN (4.1 to 5.3), indicating that the interparticle friction coefficient alone may be not enough to account for all the effects of finer particles.

The LWD loading is essentially dynamic. To find out if the model is still valid under quasi-static loading conditions, and to investigate the effects of different loading style on the simulation results, a series of simulated triaxial loading tests on the same sets of materials were carried out and the results are presented in Fig 6. To ensure a quasi-static loading, the loading rate is very slow (0.1% per second). Both loading and unloading stages were performed for each specimen. And the resilient modulus (a secant modulus, e.g., the slope of line segment AB in Fig. 6b) was estimated from the recorded data. The detailed description of the simulation of triaxial tests can be referred to [23]. Fig 6 (c) and 6 (d) show that the resilient modulus is much smaller than the LWD modulus, this is mainly due to the fact that the specimen was loaded only once comparing with 6 consecutive loadings of LWD

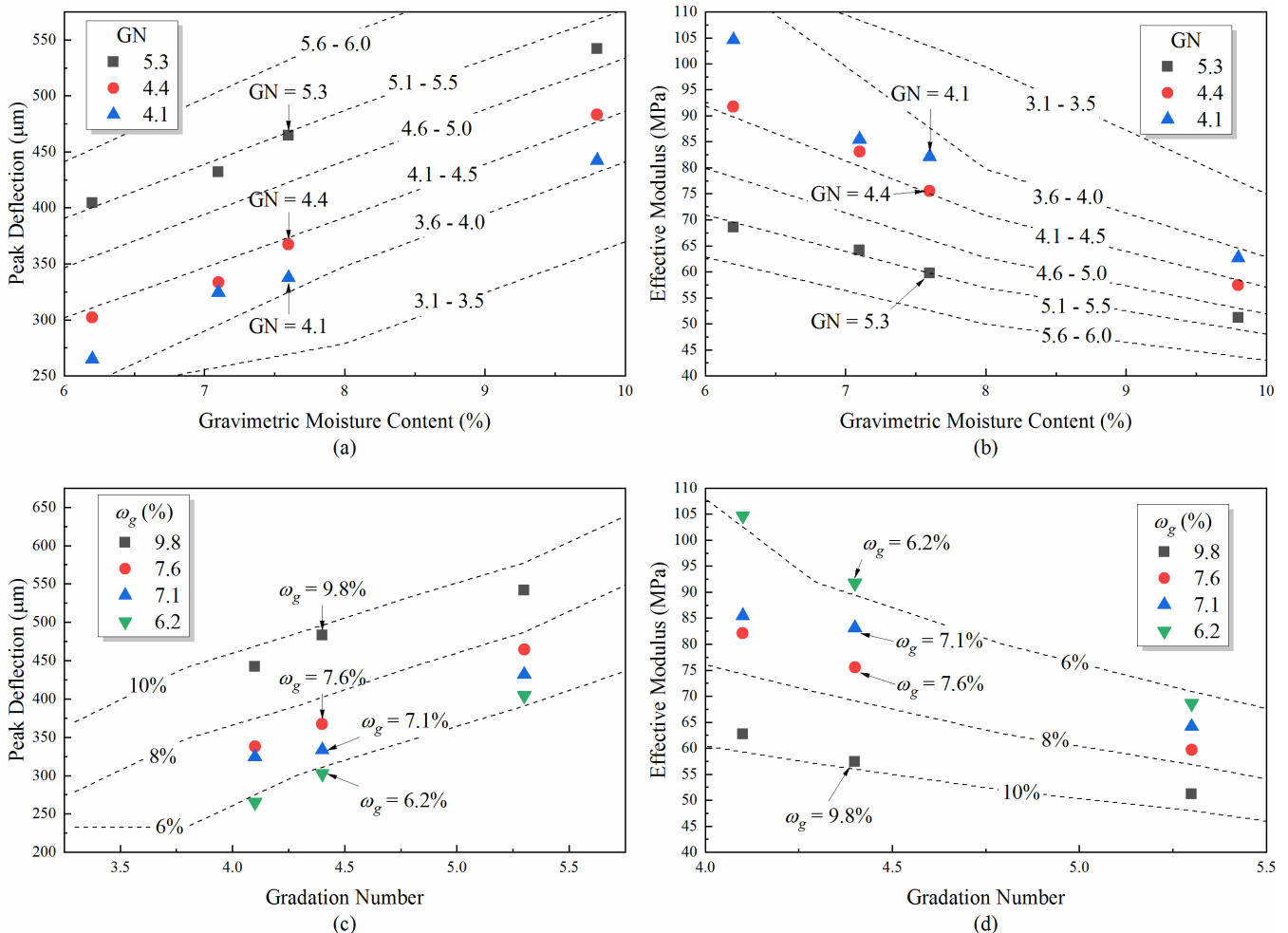


Fig. 5. Model LWD test results plotted with experimental values from [17]: (a) peak deflection and (b) corresponding bulk modulus as functions of gravimetric moisture content and (c) peak deflection and (d) corresponding bulk modulus as functions of grading number (symbols = translated model test results; dashed lines = experimental values).

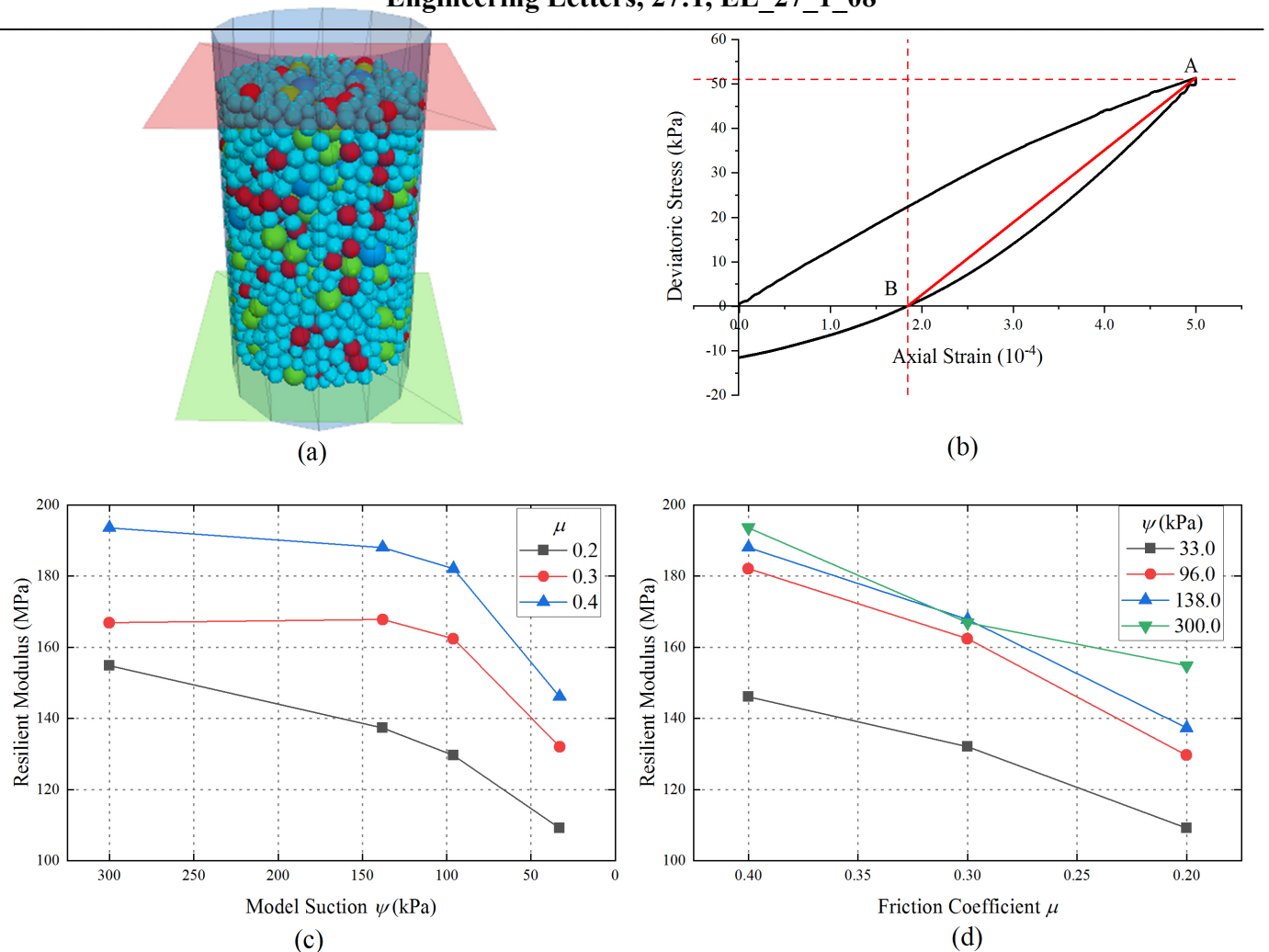


Fig. 6. Model triaxial tests and resulting resilient modulus. (a) triaxial test setup, (b) estimation of resilient modulus, (c) resilient modulus as a function of model suction, and (d) resilient modulus as a function of interparticle friction

tests. Besides the differences on magnitude, the overall trends of modulus are similar between the two types of tests.

VII. CONCLUSION

We have employed a DEM model to simulate an LWD test of G-A-5 grading material. The coarse particles were simulated explicitly, whereas finer particles were simulated via a contact model. A modified Hertz model was employed to consider the effect of moisture and fines, which are represented by interparticle suction and friction, respectively. By adopting a body-contraction scheme, we prepared dense specimens of unsaturated granular material. Several simulated LWD tests were performed on the prepared specimens. From the simulation results, the following trends were observed:

1. LWD modulus increases, or peak deflection decreases with increasing model suction. Similar trends were observed with decreasing moisture content in physical LWD tests.
2. LWD modulus increases, or peak deflection decreases with increasing interparticle friction. Similar trends were observed with decreasing fine content in physical LWD tests.

Under reasonable assumptions, the LWD test model was calibrated with published field test results from [17]. The translated results agree with experimental trends and the calibration equations can be used to predict the behavior of unbound granular material under LWD loading. Further, the results were compared with the resilient modulus obtained

from simulated triaxial tests in which a quasi-static loading condition was applied. The model well captured the deformation behavior under both conditions. Hopefully, The DEM model has the potential to be used as a possible substitute for physical experiments required for pavement design quality control. However, it should be noted the relationships between micro and macro properties presented in this paper are based upon simplified assumptions. Thus, more simulated tests need to be performed to further explore micro-macro relationships from a micro-mechanical perspective. Also, the differences of stress states and boundary conditions between the simulation and field test may lead to incorrect predictions and are not covered in this paper. To address this issue, LWD tests on mold [8] should be performed. The related tests and simulations are in progress and are deferred for future work.

REFERENCES

- [1] G. Doré and H. K. Zubeck, *Cold regions pavement engineering*. 2009.
- [2] Werkmeister S., Dawson A. R., and Wellner F., "Pavement design model for unbound granular materials," *J. Transp. Eng.*, vol. 130, no. 5, pp665–674, 2004.
- [3] A. Adu-Osei, D. Little, and R. Lytton, "Cross-anisotropic characterization of unbound granular materials," *Transp. Res. Rec. J. Transp. Res. Board*, vol. 1757, pp82–91, Jan. 2001.
- [4] M. S. Rahman, "Characterising the deformation behaviour of unbound granular materials in pavement structures," Architecture and the Built Environment, KTH Royal Institute of Technology, Stockholm, 2015.

- [5] F. Lekarp, U. Isacsson, and A. Dawson, "State of the art. I: resilient response of unbound aggregates," *J. Transp. Eng.*, vol. 126, no. 1, pp66–75, 2000.
- [6] A. Molenaar and A. van Niekerk, "Effects of gradation, composition, and degree of compaction on the mechanical characteristics of recycled unbound materials," *Transp. Res. Rec. J. Transp. Res. Board*, no. 1787, pp73–82, 2002.
- [7] Fuming Wang, Jianwei Liang, and Yunsheng Wang, "Application of portable falling weight deflectometer on the compaction quality control of soil-aggregate mixtures," *Railw. Eng.*, no. 9, pp67–70, 2008.
- [8] C. W. Schwartz, Z. Afsharikia, and S. Khosravifar, "Standardizing lightweight deflectometer modulus measurements for compaction quality assurance," Maryland. State Highway Administration, 2017.
- [9] Y. Xiao, E. Tutumluer, and Y. Qian, "DEM Approach for engineering aggregate gradation and shape properties influencing mechanical behavior of unbound aggregate materials," in *Geo-Congress 2014: Geo-characterization and Modeling for Sustainability*, 2014, pp2898–2910.
- [10] L. Uthus, M. A. Hopkins, and I. Horvli, "Discrete element modelling of the resilient behaviour of unbound granular aggregates," *Int. J. Pavement Eng.*, vol. 9, no. 6, pp387–395, Dec. 2008.
- [11] F. Alonso-Marroquín and H. J. Herrmann, "The incremental response of soils. An investigation using a discrete-element model," *J. Eng. Math.*, vol. 52, no. 1, pp11–34, Jul. 2005.
- [12] Guanhua Sun, Tan Sui, and Alexander M. Korsunsky, "Review of the Hybrid Finite-Discrete Element Method (FDEM)," Lecture Notes in Engineering and Computer Science: Proceedings of The World Congress on Engineering 2016, 29 June - 1 July, 2016, London, U.K., pp843-847.
- [13] N. Belheine, J. P. Plassiard, F. V. Donzé, F. Darve, and A. Seridi, "Numerical simulation of drained triaxial test using 3D discrete element modeling," *Comput. Geotech.*, vol. 36, pp320–331.
- [14] A. Dabeet, "Discrete element modeling of direct simple shear response of granular soils and model validation using laboratory tests," University of British Columbia, 2014.
- [15] D. Tan, L. Khazanovich, J. Siekmeier, and K. Hill, "Discrete element modeling of effect of moisture and fine particles in lightweight deflectometer test," *Transp. Res. Rec. J. Transp. Res. Board*, vol. 2433, pp58–67, Dec. 2014.
- [16] D. S. Tan, L. Khazanovich, J. Siekmeier, and K. M. Hill, "Discrete Element Modeling of the Effect of Moisture in the Light Weight Deflectometer Test Using Liquid Bridges," in *Transportation Research Board 92nd Annual Meeting*, 2013.
- [17] P. Davich, F. Camargo, B. Larsen, R. Roberson, and J. Siekmeier, "Validation of DCP and LWD moisture specifications for granular materials," 2006.
- [18] J. Siekmeier *et al.*, "Using the dynamic cone penetrometer and light weight deflectometer for construction quality assurance," 2009.
- [19] P. A. Cundall and O. Strack, "A discrete numerical model for granular assemblies," *Géotechnique*, vol. 29, no. 1, pp47–65, Jan. 1979.
- [20] M. Machado, P. Moreira, P. Flores, and H. M. Lankarani, "Compliant contact force models in multibody dynamics: Evolution of the Hertz contact theory," *Mech. Mach. Theory*, vol. 53, pp99–121, 2012.
- [21] G. Lian, C. Thornton, and M. J. Adams, "A theoretical study of the liquid bridge forces between two rigid spherical bodies," *J. Colloid Interface Sci.*, vol. 161, no. 1, pp138–147, 1993.
- [22] Sc. Gupta and W. E. Larson, "Estimating soil water retention characteristics from particle size distribution, organic matter percent, and bulk density," *Water Resour. Res.*, vol. 15, no. 6, pp1633–1635, 1979.
- [23] D. Potyondy, "Material-modeling support in PFC [fistpkg25]," Itasca Consulting Group, Technical Memo ICG7766-L, Mar. 2017.
- [24] D. Tan, K. Hill, and L. Khazanovich, "Quantifying moisture effects in DCP and LWD tests using unsaturated mechanics," Minnesota Department of Transportation Research Services & Library, MN/RC 2014-13, 2014.
- [25] A. W. Ahmed and S. Erlingsson, "Evaluation of permanent deformation models for unbound granular materials using accelerated pavement tests," *ROAD Mater. PAVEMENT Des.*, vol. 14, no. 1, pp178–195, Mar. 2013.